ATOMIC COLLISION PROCESSES RELATING TO THE IONOSPHERE*

Sponsored by Advanced Research Projects Agency

ANNUAL REPORT

Period of Report: September 1, 1969 - March 31, 1970
Effective Date of Contract: June 30, 1969
Period of Contract: September 1, 1969 - August 31, 1970

ARPA Order Number: ARPA 1482
Contract Number: DAHC04-69-C-0094
Program Code Number: 9E20
Amount: $71,000

Principal Investigators and Project Scientists: P. J. Chantry (412) 256-3675
A. V. Phelps (412) 256-7712

Unless otherwise noted, the results given in this memo should be considered as preliminary.

Arc and Plasma Research
Westinghouse Research Laboratories
Pittsburgh, Pennsylvania 15235

ATOMIC COLLISION PROCESSES RELATING TO THE IONOSPHERE*

Sponsored by Advanced Research Projects Agency

ANNUAL REPORT

Period of Report: September 1, 1969 - March 31, 1970
Effective Date of Contract: June 30, 1969
Period of Contract: September 1, 1969 - August 31, 1970

ARPA Order Number: ARPA 1482
Contract Number: DAHC04-69-C-0094
Program Code Number: 9E20
Amount: $71,000

Principal Investigators and Project Scientists: P. J. Chantry (412) 256-3675
A. V. Phelps (412) 256-7712

Unless otherwise noted, the results given in this memo should be considered as preliminary.

Arc and Plasma Research
Westinghouse Research Laboratories
Pittsburgh, Pennsylvania 15235

ABSTRACT

This annual report for Contract DAHC04-69-C-0094 contains an account of work performed during the initial seven months (September 1, 1969 - March 31, 1970) of the current contract period. Measurements of the attachment cross sections in O_3 reveal no dependence on temperature below 361°K in the energy range 0-4 eV. Measurements of the momentum transfer cross section Q_m in N_2, required for the deduction of the total inelastic collision cross section ΣQ_x from the product $Q_m \Sigma Q_x$ measured by a high pressure beam technique, show serious discrepancies with published data. Possible reasons for this are discussed.

TABLE OF CONTENTS

1. INTRODUCTION

This annual report is an account of work being performed under Contract DAHC04-69-C-0094, ARPA Order No. 1482, administered by the Army Research Office, Durham. The total program for the current contract period, September 1, 1969 to August 31, 1970, consists of experimental measurements of (i) total inelastic collision cross sections in N_2 and O_2, and (ii) the temperature dependence of attachment cross sections in O_3. Our progress during the initial seven months of this contract period is reported in Section 2; progress anticipated by the end of the current contract and related work which it is hoped will form part of a proposed continuation of the present contract, are summarized in Section 3.

The experimental work described herein has been performed by P. J. Chantry, with the participation of A. V. Phelps in the planning and interpretation of the experiments.

2. TECHNICAL ACCOMPLISHMENTS

2.1 Temperature Dependence of Electron Attachment in Ozone

2.1.1 Experiment

The apparatus used for this experiment is basically the same as was used previously[1] in the measurement of the attachment cross sections at room temperature. For the present work it was, however, necessary to rebuild the tube to permit control of the collision chamber temperature. To this end the collision chamber was manufactured from a solid block of stainless steel which was bolted to the base of a specially constructed dewar vessel. This arrangement is shown in Fig. 1. The system of electrodes comprising the electron gun and collector (not shown) and that comprising the Wien filter are mounted directly from the collision chamber block so that the only physical connection to the whole tube is via the dewar and the electrical leads. The latter are of thin wire and thus provide negligible heat conduction.

The fluids used in turn to control the collision chamber temperature were liquid nitrogen, solid CO_2 in acetone, air (dewar empty), and hot oil. In each case the temperature was monitored at two points: at the base of the dewar and at the base of the collision chamber, by an internal thermocouple. The three walls of the chamber not required to transmit ions or electrons were made much thicker than the remainder in order to provide a reasonably isothermal enclosure.

Gas was admitted to the chamber through one of the two metal tubes which pass down the center of the dewar vessel. The second of these tubes was connected to a Baratron[2] absolute pressure gauge used to monitor the collision chamber pressure. This arrangement provided pre-cooling (or heating) of the gas before it entered the chamber.

---

1. Final Report, Contract NONR-2584(00 ARPA 125, September 1968.
2. MKS Instruments, Burlington, Massachusetts.

That the gas was indeed reaching a temperature corresponding to that indicated by the measured temperatures was checked by a method described below.

Details of the operation of this tube have been given previously[3,4,5] and are only outlined here. The electron beam (EB) is produced by a series of electrodes which permit the use of the Retarding Potential Difference (RPD)[6] technique for reducing the effective energy spread of the beam. In the present work a resolution of approximately 0.1 eV was achieved. The beam is aligned by a magnetic field of approximately 200 gauss which also serves the Wien Filter. Within the collision chamber the electron beam passes midway between the parallel Repeller (Rep) and Attractor (Attr) plates. These impose a transverse electric field which causes the ions produced in the chamber to travel to one or other of these plates. The current to the appropriate plate is monitored and provides a measure of the total rate of ion production in the chamber. The corresponding cross section is determined from a simultaneous measurement of the gas pressure in the collision chamber, having calibrated the system by similar observations of an ionization process whose cross section is known.

With the appropriate direction of the ion extraction field a small sample of the positive or negative ions produced in the collision chamber pass through the slit in the attractor. This slit forms the entrance slit of the Wien filter which selectively transmits ions having velocity E/B where E is the electric field applied between the parallel plates of the filter. By scanning the ion accelerating voltage applied between the collision chamber and the filter one obtains the ion kinetic energy spectrum. On leaving the Wien filter, the ions pass into the mass spectrometer where they are detected by a channeltron[7]

3. P. J. Chantry and G. J. Schulz, Phys. Rev. 156, 134 (1967).
4. P. J. Chantry, Phys. Rev. 172, 125 (1968).
5. P. J. Chantry, J. Chem. Phys. 51, 3369 (1969).
6. R. E. Fox, W. M. Hickam, T. Kjeldaas and D. J. Grove, Rev. Sci. Instr. 26, 1101 (1955).
7. Bendix Corporation, Ann Arbor, Michigan.

multiplier. The output pulses are counted by conventional techniques, or fed to a multichannel scaler used to automatically accumulate RPD data as a function of electron or ion energy.[8]

2.1.2 Results

The temperatures measured at the base of the dewar (T_1) and at the base of the collision chamber (T_2) with various fluids are shown in Table I. Measurements of attachment to ozone were not possible at

Table I. Temperatures measured at the base of the dewar (T_1) and at the base of the collision chamber (T_2) with various fluids in the dewar.

Fluid	T_1°K	T_2°K	Mean
Liquid N_2	78	146	112
Solid CO_2	198	223	210
Empty	356	367	361
Hot Oil	492	455	473

the highest temperature shown, due to essentially complete conversion of the O_3 to O_2. At 361°K and lower temperatures no variation in the shapes or the magnitudes of the cross sections for O^- and O_2^- production from O_3 were detected for electron energies 0-4 eV. The above conclusion is only valid if the gas sampled by the electron beam is in temperature equilibrium with the collision chamber. Calculations performed for a different system[9] suggest that in the present system the gas would have more than adequate time to reach equilibrium due to the long pre-cooling tube through which it is admitted. In order to confirm that the gas has a translational temperature corresponding to the measured collision chamber temperature measurements were made of the

8. P. J. Chantry, Rev. Sci. Instr. 40, 884 (1969).
9. See Section II D of Ref. 5.

BLANK PAGE

positive ion current to the repeller as a function of the Baratron reading using O_2 and 110 eV electrons. The results are shown in Fig. 2 where the temperatures shown correspond to the mean temperatures listed in Table I. One may show that, if the temperature of the gas in the Baratron sensing head is constant and the transport of gas between the Baratron and the collision chamber is dominated by molecule-wall collisions, then the number density N of gas molecules in the collision chamber is related to the pressure p(Bar) read by the Baratron by the equation

$$N = \frac{Ap(Bar)}{T_{cc}^{1/2}}$$

where A is constant. Thus, referring to Fig. 2, the ion currents detected at temperatures T_1, T_2, T_3°K, at the same Baratron pressure, should be in the ratio $1:(T_1/T_2)^{1/2}:(T_1/T_3)^{1/2}$. According to the measured mean temperatures these ratios should be 1:0.73:0.55. The ratios read from Fig. 2 are 1:0.72:0.56. We may therefore conclude that the translational temperature of the gas is very close to the measured mean temperature of the collision chamber. This is consistent with our belief that the gas is in thermal equilibrium, vibrational and rotational as well as translational, at the collision chamber temperature.

As stated above, no temperature dependence of the attachment cross section was detected within the range of temperatures studied. The cross sections are shown in Fig. 3 which is a reproduction of the room temperature data obtained previously.[1] In searching for a possible temperature dependence of the attachment cross sections particular emphasis was placed on studying the energy region below 1.0 eV, since our experience with other gases suggests that such effects are likely to be most pronounced at low electron energies, and be most easily detected at the threshold of the process of interest.

We were particularly interested in any temperature dependence of the threshold for O_2^- production, since in principle this provides an upper limit for D-A where D is the strength of the O_2-O bond and A

is the affinity of O_2. Since D is well known[10] (D = 1.0 eV), one thereby deduces a lower limit for A. The values of $A(O_2) \gtrsim 0.58$ eV, deduced by Curran[11] from the threshold of O_2^- from O_3, and of $A(O_2) \gtrsim 1.1$ eV deduced by Stockdale et al.[12] from similar measurements in NO_2, are of questionable validity since neither study demonstrated that the threshold was independent of gas temperature. The observation in the present work that the O_2^- from O_3 threshold is insensitive to temperature below 360°K suggests that the threshold measured here and by Curran[11] should agree, and should provide a valid lower limit to the affinity of O_2.

By using a linear extrapolation of the leading edge of the present O_2^- data a threshold of 0.40 eV is obtained with a precision of ± 0.05 eV. This is in good agreement with the value quoted by Curran. The absolute accuracy of this threshold is, however, somewhat less than the quoted precision because the detailed shape of the cross section in the threshold region is unknown, and the exact procedure to be adopted in determining the threshold from the data is undetermined. Thus the confidence limits to be placed on the measured threshold should probably be somehwat wider than would be the case if the cross section were known to rise linearly, or vertically from threshold.[13] The linear extrapolation used in the present circumstances is, however, unlikely to introduce a systematic error greater than 0.1 eV, and we place an overall confidence limit of ± 0.15 eV on the threshold determination. Thus we deduce that the electron affinity A of O_2 is $A \gtrsim 0.60 \pm 0.15$ eV. Thus, there is a marginal discrepancy between this value and the presently preferred value of 0.43 ± 0.02 eV determined by Pack and Phelps.[14]

---

10. G. Herzberg, Molecular Spectra and Molecular Structure III (D. Van Nostrand, Inc., New York, 1966).
11. R. K. Curran, J. Chem. Phys. 35, 1849 (1961).
12. J. A. D. Stockdale, R. N. Compton, G. S. Hurst and P. W. Reinhardt, J. Chem. Phys. 50, 2176 (1969).
13. For a discussion of the data analysis applicable to such cases, see Ref. 4.
14. J. L. Pack and A. V. Phelps, J. Chem. Phys. 44, 870 (1966).

The magnitude of the cross sections reported previously[1] have since been remeasured, and leads to only a minor change. The cross section at the peak of the total cross section is revised from $(2.8 \pm 0.7) \times 10^{-17}$ cm^2 to $(3.0 \pm {}^{0.7}_{0.4}) \times 10^{-17}$ cm^2. More recent determinations of the ratios of the various cross sections at their peaks Q_a:$Q(O^-/O_3)$: $Q:(O_2^-/O_3)$ confirm the values quoted previously,[1] i.e., 1.6:1:0.75.

The only quantitative data with which these cross sections can be compared is that obtained in swarm experiments. In reference 1 a serious discrepancy between the electron beam data and the preliminary swarm data of Moruzzi and Phelps[15] was noted. A similar approximate comparison of the electron beam data with the more recent swarm data of Stelman and Phelps[16], however, shows sufficiently close agreement to warrant a more detailed comparison. Preliminary results show that there is satisfactory agreement between the magnitude of the electron beam total cross section and the swarm data at the highest energies probed in the swarm experiment (~ 0.8 eV), but that at very low energies (< 0.1 eV) the swarm data requires a cross section which is very small, rising approximately linearly with energy. Such a cross section is shown by the broken curve at energies < 0.5 eV in Fig. 3.

2.2 Total Inelastic Collision Cross Sections

The only technique previously used for the measurement of total inelastic collision cross sections is that developed by Maier-Leibnitz.[17] In view of the difficulties associated with the interpretation[18] of this type of experiment, and its limited energy range, we have developed a new technique by which to determine such cross sections. It is based on the theoretically predicted[18] behavior of mono-energetic electrons injected into a scattering chamber in which the gas pressure may be varied from 10^{-5} Torr to greater than 10^{-1} Torr. Under these conditions the local density of electrons retaining the energy ε with

15. J. L. Moruzzi and A. V. Phelps, Bull. Amer. Phys. Soc. 13, 209 (1968).
16. Final Report, Contract F29601-68-C-0070, June 1969.
17. H. Maier-Leibnitz, Z. Physik 95, 499 (1935).
18. P. J. Chantry, A. V. Phelps and G. J. Schulz, Phys. Rev. 152, 81 (1966).

which they were injected into the cell is a calculable function of the momentum transfer cross section $Q_m(\varepsilon)$ and the total inelastic collision cross section $\Sigma Q_x(\varepsilon)$. Thus, by ensuring that the technique used to sense the local electron density discriminates against those electrons which have lost energy, we have a method for determining $\Sigma Q_x(\varepsilon)$, provided Q_m is known or can be measured. The measurement of the production rate of ions (positive or negative) fulfills this criterion provided A.P. $< \varepsilon \leq$ A.P. + ε_1^* where AP is the appearance potential of the ion and ε_1^* is the lowest relevant excitation energy.

The apparatus employed in this study is shown in Fig. 4. The length of the scattering chamber, i.e., the separation of the entrance and exit grids, is 10.0 cm. The electron beam enters the chamber through the 0.020" diam. aperture in the entrance plate. At low chamber pressures the beam travels up the tube midway between the parallel plates and is collected by electron collector 2 (EC_2). Alignment of the applied axial magnetic field of 700 gauss is achieved by minimizing the current collected by EC_1 under vacuum conditions. Having aligned the beam, EC_1 and EC_2 are connected together, the total current being monitored thereafter. The method of operating the tube depends on the type of measurement being made.

2.2.1 Measurement of $Q_m \Sigma Q_x$

In measuring $Q_m \Sigma Q_x$ a field of typically 6 V/cm is applied between the parallel plates so as to extract the ions formed on axis to the adjacent portion of that plate containing the mesh covered holes. Ions passing through these mesh covered holes are accelerated further and collected by the small plates C_1, C_2, C_3. In this way the local rates of ionization at these three positions along the electron beam are monitored. The ratios of the currents C_1/C_3; C_1/C_2; C_2/C_3 are measured as a function of pressure at various electron energies satisfying the criterion given above.

The data analysis may be illustrated by the following simple example, corresponding to operation of the tube at the highest usable pressures. In this case the electron beam is essentially completely

scattered shortly after entering the chamber. The density of electrons retaining energy ε at greater distances is then of the form[19]

$$n(x) = n(o) \exp\left[- S \frac{x}{L}\right] \tag{1}$$

where

$$S = NL \sqrt{3\, Q_m \Sigma Q_x} \tag{2}$$

N = gas particle density

L = chamber length

Thus the ratio of electron densities responsible for the ion currents to, for example, C_1 and C_2, behaves as $\exp\left[(3\, Q_m \Sigma Q_x)^{1/2} N(x_2 - x_1)\right]$ where x_1 and x_2 are the positions of C_1 and C_2. If ΔN is the measured change in density required to change this ratio by e, then

$$Q_m \Sigma Q_x = \frac{3}{(\Delta N^2)\,(x_2 - x_1)^2} \tag{3}$$

We note that the only absolute measurements involved are N (i.e., the gas pressure) and distances.

The above relationship (3) is applicable only at the highest pressures used in the present studies. In practice use is made of data taken over the whole pressure range by fitting the whole curve to curves computed from the more complicated theoretical expressions valid for the whole pressure range. Such curves are shown in Fig. 5. It is clear from this figure that the shape of the curve is rather insensitive to the ratio $\Sigma Q_x/(Q_m + \Sigma Q_x)$, so that it is difficult from such curves to determine Q_m and ΣQ_x separately. Moreover, interpretation of the detailed shape is complicated by its sensitivity to the boundary conditions, shown in Fig. 6. We note, however, that in the region $S > 6$

19. Compare with Eq. 3.11 in Ref. 18. The parameter S used here, Eq. (1), is a generalized form of the parameter q used in Ref. 18. The equation for S used here (Eq. 2) is an approximation which is accurate to 2% provide $\Sigma Q_x \leq Q_m/4$.

the curves are insensitive to the boundary conditions. This is an important advantage of the technique.

In the most recent version of the experimental tube (Fig. 4) we have attempted to control these reflection coefficients by introduction of the entrance and exit grids, allowing the electrons approaching the entrance plate or electron collector to be accelerated onto the surfaces, which are plated with platinum black. However, in making the measurements of ion currents to C_1, C_2, and C_3, it is found necessary to restrict the accelerating voltages between the entrance grid and entrance plate, and between the exit grid and electron collector, to no more than a few volts in order not to cause significant ion production in these regions. Thus control over the reflection coefficients is limited, and a direct interpretation of the ratio curves in the region of S = 1 is not possible. The above considerations do not, however, significantly affect the interpretation of the data above S = 6 from which we obtain $Q_m \Sigma Q_x$. From this we may deduce ΣQ_x using Q_m values from the literature or from an independent determination of Q_m, as discussed below.

2.2.2 Measurement of Q_m

As discussed above, in order to obtain values of $\Sigma Q_x(\varepsilon)$ from the ion current ratio measurements we need to know $Q_m(\varepsilon)$. The values available in the literature for N_2[20] and O_2[21] were obtained in the range of energy of interest here by adjusting measured total collision cross sections to provide agreement between computed and measured transport coefficients. This procedure is in general a sensitive test of the momentum transfer cross section at energies corresponding to the range of mean electron energies covered by swarm experiments. Thus, these studies[20,21] do not provide accurate data of most of the energies of interest in the present work (4-20 eV).

---

20. A. G. Engelhardt, A. V. Phelps and C. G. Risk, Phys. Rev. 135, A1566 (1964).

21. R. D. Hake and A. V. Phelps, Phys. Rev. 158, 70 (1967).

In view of this situation an effort has been made to determine Q_m by direct experiment using the same apparatus as used in the ion current ratio measurements. In this case attention is focussed on the fraction of the injected electron current which is transmitted to the electron collector as a function of pressure. The dependence may be theoretically predicted essentially exactly as a function of NQ_mL, so that by matching the computed curve to the measured pressure dependence the value of Q_m may be deduced. Examples of this type of data are shown in Fig. 7 where Xe was chosen to provide a test of the experiment over a wide range of Q_m. It was found necessary to take into account the electron current collected by the exit grid. Though negligible at low pressures, this represented approximately 40% of the total when the transmitted current was reduced to 5% of its vacuum level by gas scattering. The experimental points plotted in Fig. 7, representing the sum of the currents measured at the exit grid and the electron collectors, show an excellent fit to the theoretically predicted shape of the curve, shown by the full lines.

The dependence on electron energy of Q_m obtained from measurements of this type in Xe and N_2 are shown in Figs. 8 and 9. Comparison of the present data with other available data[20,22,23,24] suggests that the present data may be consistently low at high energies but satisfactory at low energies (~ 1 eV). Data taken in other gases (Ar,He) supports this hypothesis, but the limited accuracy of the literature data on Q_m at the higher energies precludes a definite conclusion regarding the cause of the discrepancies.

In order to check on certain of the measured quantities entering into the determination of Q_m, a number of measurements were made of the total collision cross section, for direct comparison with other beam data. In the present apparatus such measurements are done by

22. L. S. Frost and A. V. Phelps, Phys. Rev. 136, A1538 (1964).
23. G. L. Braglia, Physics Letters 17, 260 (1965).
24. K. Takayanagi, private communication.

retarding the electrons as they approach $EC_{1,2}$, so that only those electrons which have retained their initial axial velocity can be collected. With this arrangement the collected current behaves as

$$I_c = I_o \exp [- NQ_T L]$$

over a sufficiently large range of pressure for Q_T to be measurable from a semi-logarithmic plot of I_c/I_o vs p. The results of such measurements are shown by solid squares in Figs. 8 and 9, and are to be compared with the data of Ramsauer[25] in Fig. 8 and the data of Brode[26] in Fig. 9. The agreement is seen to be satisfactory over the whole energy range, suggesting that no significant errors are entering the present Q_m data from the measurement of N (i.e., pressure) and L, the chamber length.

The discrepancies observed in Q_m may quite reasonably be ascribed to an energy dependent, non zero reflection coefficient R for electrons backscattered to the entrance plate of the chamber. If $R \neq 0$ the values of Q_m, deduced from the measurements with the assumption that $R = 0$ will be consistently low. However, efforts to vary R by varying the energy with which the backscattered electrons impinge on the inner surface of the entrance plate had little or no effect on the data. It is therefore believed that, if the present measurements are in error through $R \neq 0$, then the source of the problem lies in those back-scattered electrons which leave the scattering chamber through the entrance aperture, and are subsequently reflected back into the chamber by the field which accelerates the primary beam electrons. The simplest way to check on, and hopefully overcome this effect, would be to significantly reduce the size of the aperture in the entrance plate. Unfortunately, this would reduce the injected electron beam current to a level at which satisfactory ion current measurements are precluded, and thus cannot be tried until the measurements of $Q_m \Sigma Q_x$ are completed.

---

25. C. Ramsauer and R. Kollath, Ann. Physik 12, 837 (1932).
26. R. B. Brode, Rev. Mod. Phys. 5, 257 (1933).

3. FUTURE WORK

In Section 2 of this report we have presented the results obtained during the first seven months of the current contract. We are currently collecting data for the determination of $Q_m \Sigma Q_x$ in N_2, to be followed by similar measurements in O_2. It is anticipated that this work will be completed during the current contract. As part of a proposed program for the continuation of the current contract through August 1971 it is hoped that the accuracy achievable in the values of ΣQ_x deduced from the measured $Q_m \Sigma Q_x$ may be significantly improved by performing more accurate direct measurements of Q_m in N_2 and O_2.

During the remainder of the current contract a further attempt will be made to obtain attachment data in O_3 at temperatures above 400°K. The conversion of O_3 to O_2 which frustrated previous attempts to operate at such temperatures may however be found unavoidable.

4. PUBLICATIONS AND PRESENTATIONS SINCE SEPTEMBER 1, 1969

The following is a list of publications describing work performed under the current or previous related contracts which have appeared in various scientific publications since September 1, 1969. Also shown are the titles of oral presentations which have been made.

(i) "Temperature Dependence of Dissociative Attachment in N_2O", by P. J. Chantry, J. Chem. Phys. 51, 3369 (1969).

(ii) "Formation of N_2O^- via Ion-Molecule Reactions in N_2O", by P. J. Chantry, J. Chem. Phys. 51, 3380 (1969).

(iii) "Spurious Dissociative Attachment Peaks from Inelastic Energy Loss Reactions", by P. J. Chantry, Bull. Amer. Phys. Soc. II15, 418 (1970).

(iv) "Temperature Dependence of SF_6^-, SF_5^-, and F^- Production from SF_6", by C. L. Chen and P. J. Chantry, Bull. Amer. Phys. Soc. II15, 418 (1970).

Items (iii) and (iv) are abstracts of oral presentations made at the 22nd Gaseous Electronics Conference, Gatlinburg, Tennessee, 1969.

REFERENCES

1. Final Report, Contract NONR-2584(00) ARPA 125, September 1968.
2. MKS Instruments, Burlington, Massachusetts.
3. P. J. Chantry and G. J. Schulz, Phys. Rev. 156, 134 (1967).
4. P. J. Chantry, Phys. Rev. 172, 125 (1968).
5. P. J. Chantry, J. Chem. Phys. 51, 3369 (1969).
6. R. E. Fox, W. M. Hickam, T. Kjeldaas and D. J. Grove, Rev. Sci. Instr. 26, 1101 (1955).
7. Bendix Corporation, Ann Arbor, Michigan.
8. P. J. Chantry, Rev. Sci. Instr. 40, 884 (1969).
9. See Section II D of Ref. 5.
10. G. Herzberg, Molecular Spectra and Molecular Structure III (D. Van Nostrand, Inc., New York, 1966).
11. R. K. Curran, J. Chem. Phys. 35, 1849 (1961).
12. J. A. D. Stockdale, R. N. Compton, G. S. Hurst and P. W. Reinhardt, J. Chem. Phys. 50, 2176 (1969).
13. For a discussion of the data analysis applicable to such cases, see Ref. 4.
14. J. L. Pack and A. V. Phelps, J. Chem. Phys. 44, 870 (1966).
15. J. L. Moruzzi and A. V. Phelps, Bull. Amer. Phys. Soc. 13, 209 (1968).
16. Final Report, Contract F29601-68-C-0070, June 1969.
17. H. Maier-Leibnitz, Z. Physik 95, 499 (1935).
18. P. J. Chantry, A. V. Phelps and G. J. Schulz, Phys. Rev. 152, 81 (1966).
19. Compare with Eq. 3.11 in Ref. 18. The parameter S used here, Eq. (1), is a generalized form of the parameter q used in Ref. 18. The equation for S used here (Eq. 2) is an approximation which is accurate to 2% provide $\Sigma Q_x \leq Q_m/4$.

20. A. G. Engelhardt, A. V. Phelps and C. G. Risk, Phys. Rev. 135, A1566 (1964).

21. R. D. Hake and A. V. Phelps, Phys. Rev. 158, 70 (1967).

22. L. S. Frost and A. V. Phelps, Phys. Rev. 136, A1538 (1964).

23. G. L. Braglia, Physics Letters 17, 260 (1965).

24. K. Takayanagi, private communication.

25. C. Ramsauer and R. Kollath, Ann. Physik 12, 837 (1932).

26. R. B. Brode, Rev. Mod. Phys. 5, 257 (1933).

FIGURE CAPTIONS

Fig. 1 - The variable temperature collision chamber apparatus used in the ozone measurements, showing the electron beam (EB), the attractor (Attr) and repeller (Rep) plates and the internal thermocouple (TC).

Fig. 2 - The positive ion current in O_2 measured at the repeller as a function of Baratron reading at the measured mean collision chamber temperatures shown. The experimental points are shown only for curve 2.

Fig. 3 - The attachment cross sections in ozone. The peak total cross section (Q_a) is $(3.0 \pm {}^{0.7}_{0.4}) \times 10^{-17}$ cm^2. The shapes and relative magnitudes of the cross sections for O^- and O_2^- production were determined mass spectrometrically as described in the text. The sum of these agrees with the measured total cross section below 1.2 eV, and is indicated by the broken curve at higher energies. The broken curve below 0.5 eV is the adjustment of the total cross section required to give agreement with swarm measurements.

Fig. 4 - The high pressure electron beam tube, showing the Baratron pressure gauge (Bar), electron collectors (EC), ion collectors $C_{1,2,3}$, gas reservoirs ($G_{1,2}$) and leak valves (LV).

Fig. 5 - Computed curves for the variation with pressure of the ratio of the ion currents to collectors C_1 and C_2. The variable s is proportional to pressure and given approximately by Eq. 2 in the text. By matching the experimental points to such curves, as shown, the product $Q_m \Sigma Q_x$ is determined from the relationship of the pressure and s scales.

Fig. 6 - The dependence of the computed ion ratio on pressure for the case $\Sigma Q_x/(Q_m + \Sigma Q_x) = 0.1$ showing the dependence of the shape on the reflection coefficients R, R' at the entrance and exit boundaries.

Fig. 7 - Pressure dependence of the transmitted electron current in Xe at the energies indicated. The positions of the exact computed curves relative to the pressure scale are chosen to best fit the data, and serve to determine Q_m at each energy.

Fig. 8 - The momentum transfer (Q_m) and total (Q_T) cross sections in Xe, as determined in the present work and by previous workers. See discussion in text regarding the discrepancies.

Fig. 9 - The momentum transfer (Q_m) and total (Q_T) cross sections in N_2. The curve labelled EPR is from Ref. 20. See discussion in text regarding the discrepancies.

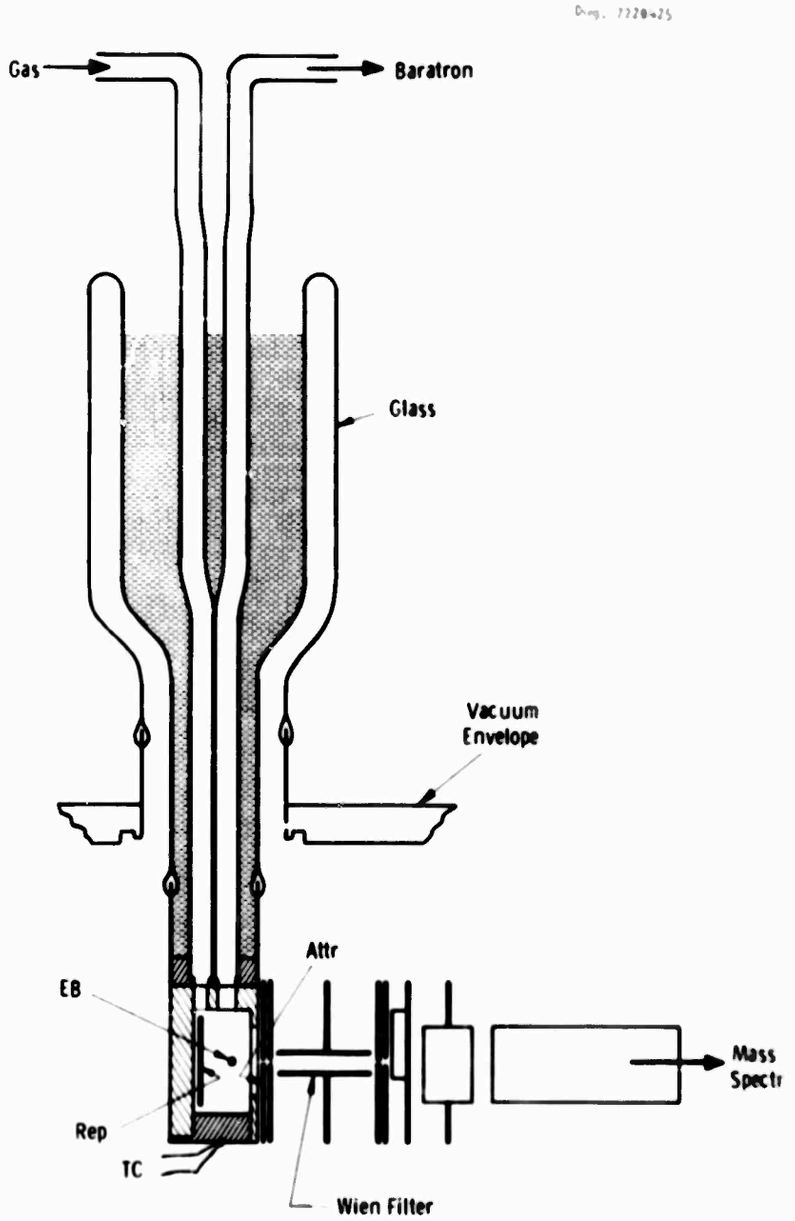

Fig. 1 - The variable temperature collision chamber apparatus used in the ozone measurements, showing the electron beam (EB), the attractor (Attr) and repeller (Rep) plates and the internal thermocouple (TC).

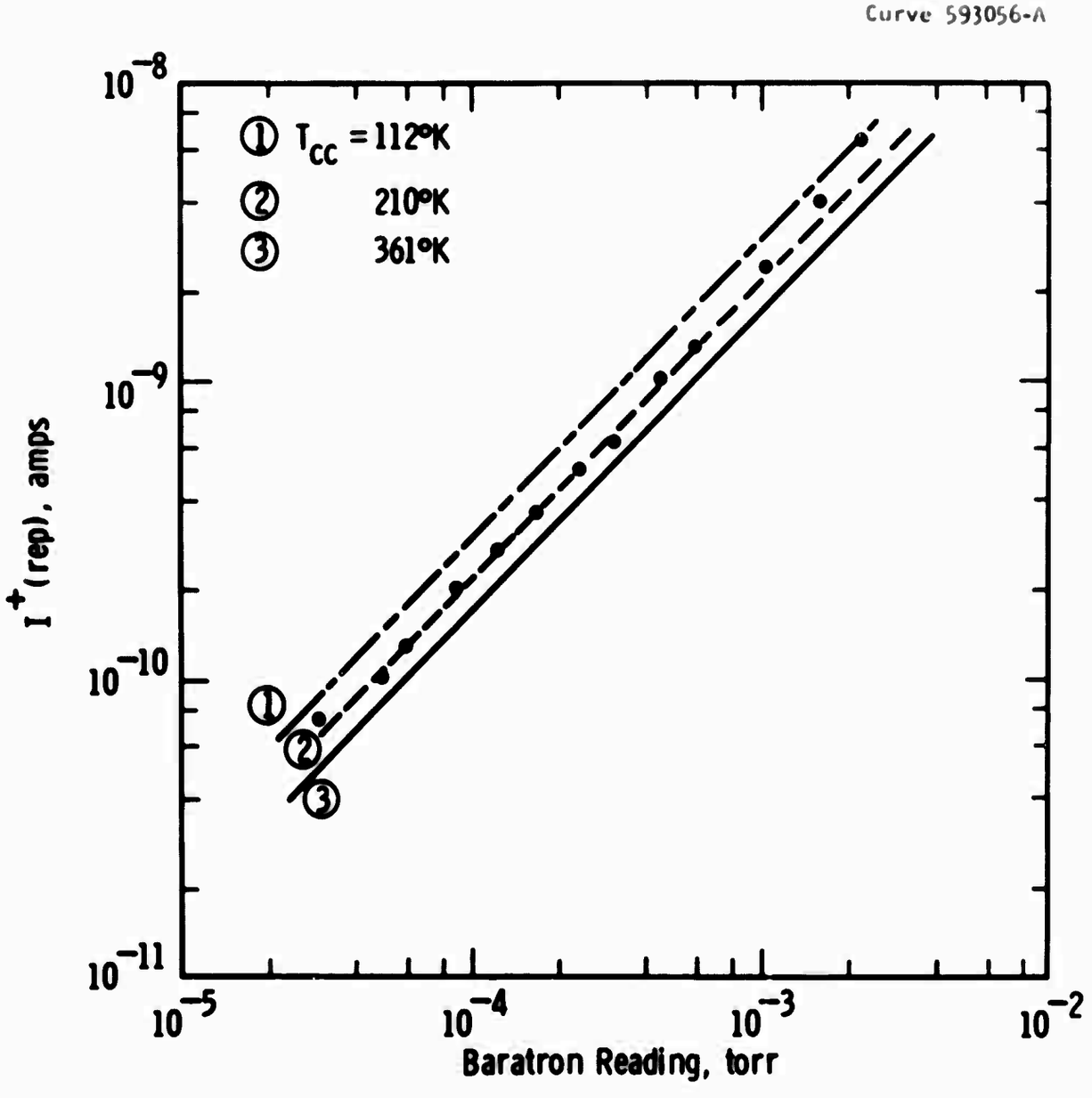

Fig. 2 - The positive ion current in O_2 measured at the repeller as a function of Baratron reading at the measured mean collision chamber temperatures shown. The experimental points are shown only for curve 2.

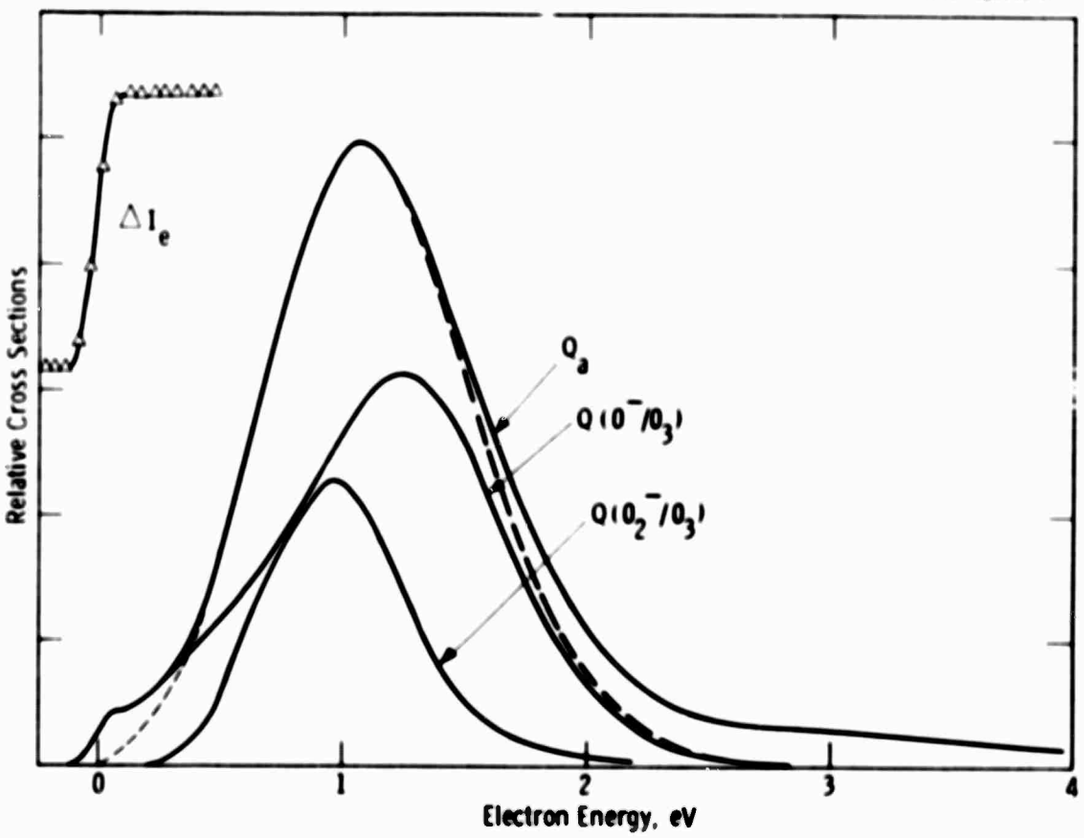

Fig. 3 - The attachment cross sections in ozone. The peak total cross section (Q_a) is $(3.0 \pm {}^{0.7}_{0.4}) \times 10^{-17}$ cm^2. The shapes and relative magnitudes of the cross sections for O^- and O_2^- production were determined mass spectrometrically as described in the text. The sum of these agrees with the measured total cross section below 1.2 eV, and is indicated by the broken curve at higher energies. The broken curve below 0.5 eV is the adjustment of the total cross section required to give agreement with swarm measurements.

Dwg. 2918A25

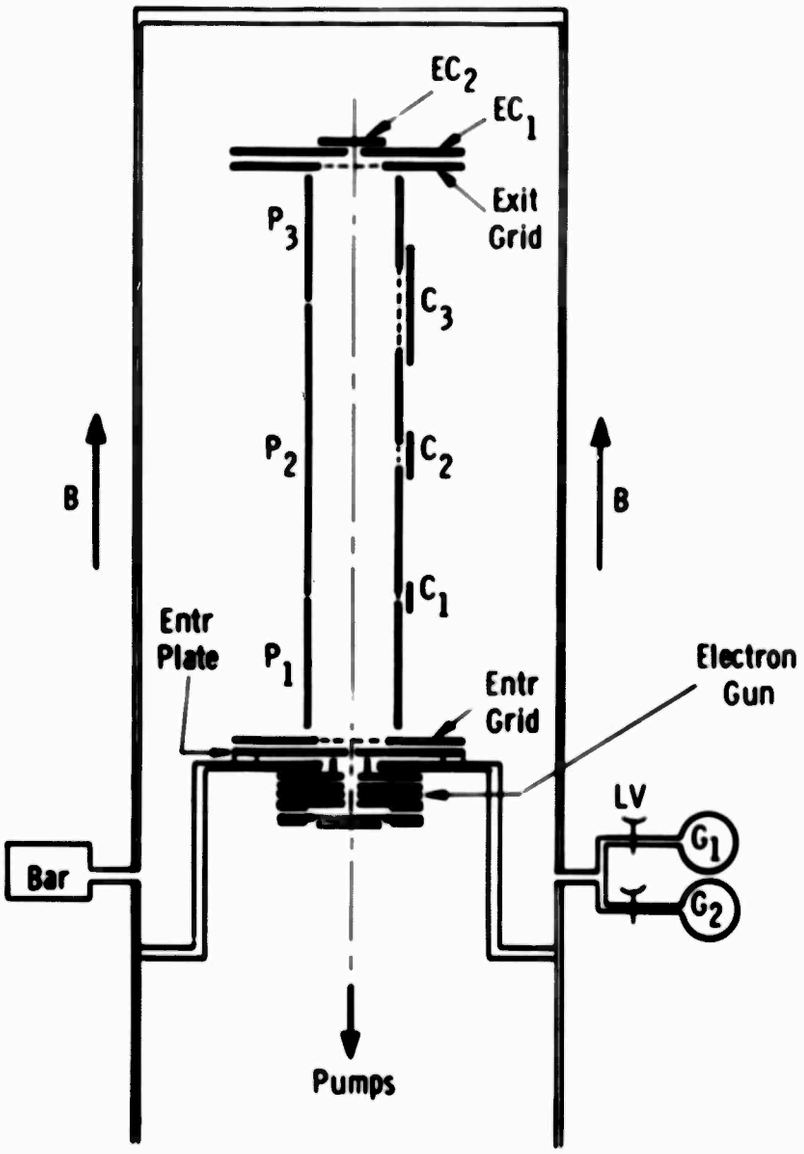

Fig. 4 - The high pressure electron beam tube, showing the Baratron pressure gauge (Bar), electron collectors (EC), ion collectors $C_{1,2,3}$, gas reservoirs ($G_{1,2}$) and leak valves (LV).

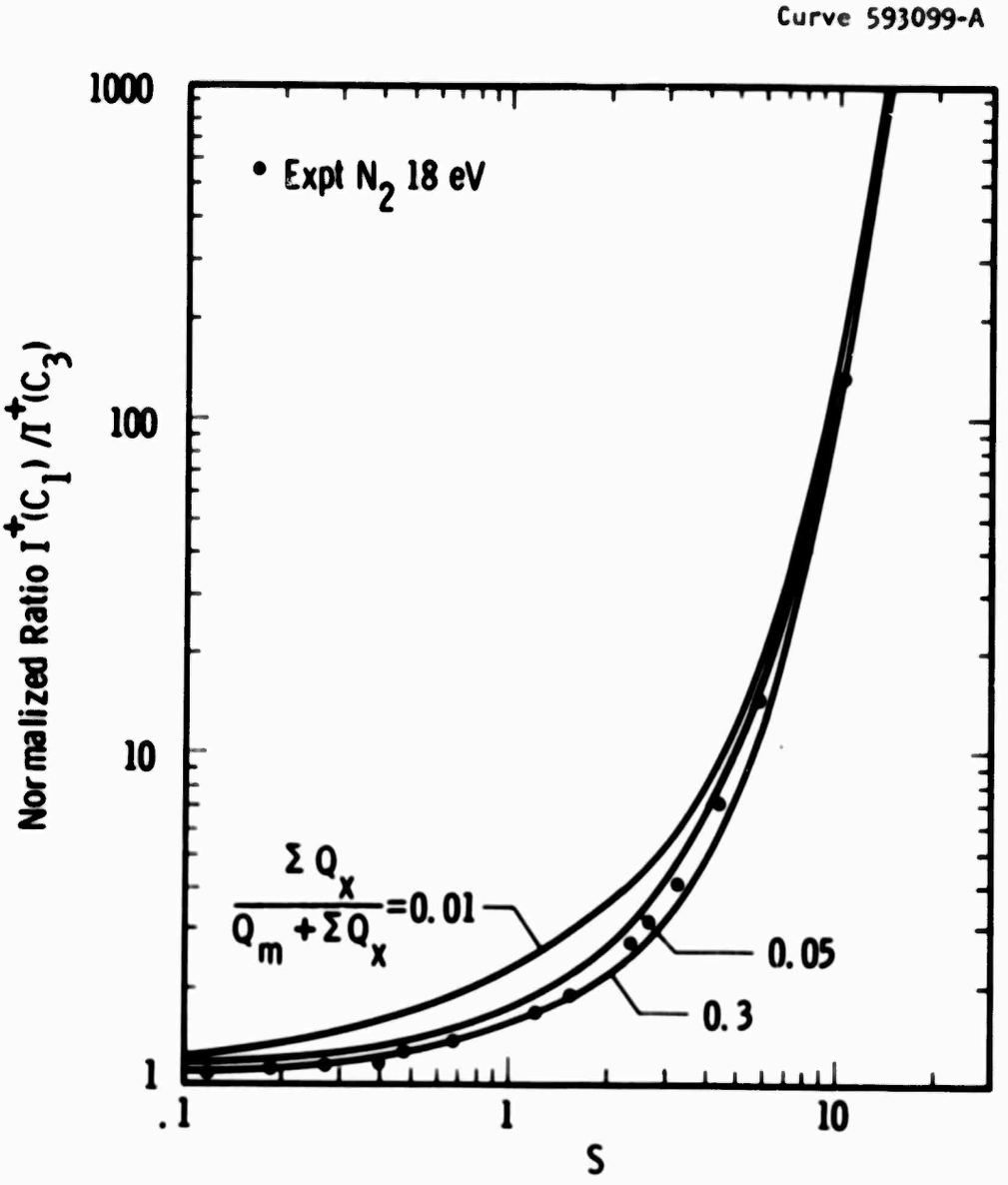

Fig. 5 - Computed curves for the variation with pressure of the ratio of the ion currents to collectors C_1 and C_2. The variable s is proportional to pressure and given approximately by Eq. 2 in the text. By matching the experimental points to such curves, as shown, the product $Q_m \Sigma Q_x$ is determined from the relationship of the pressure and s scales.

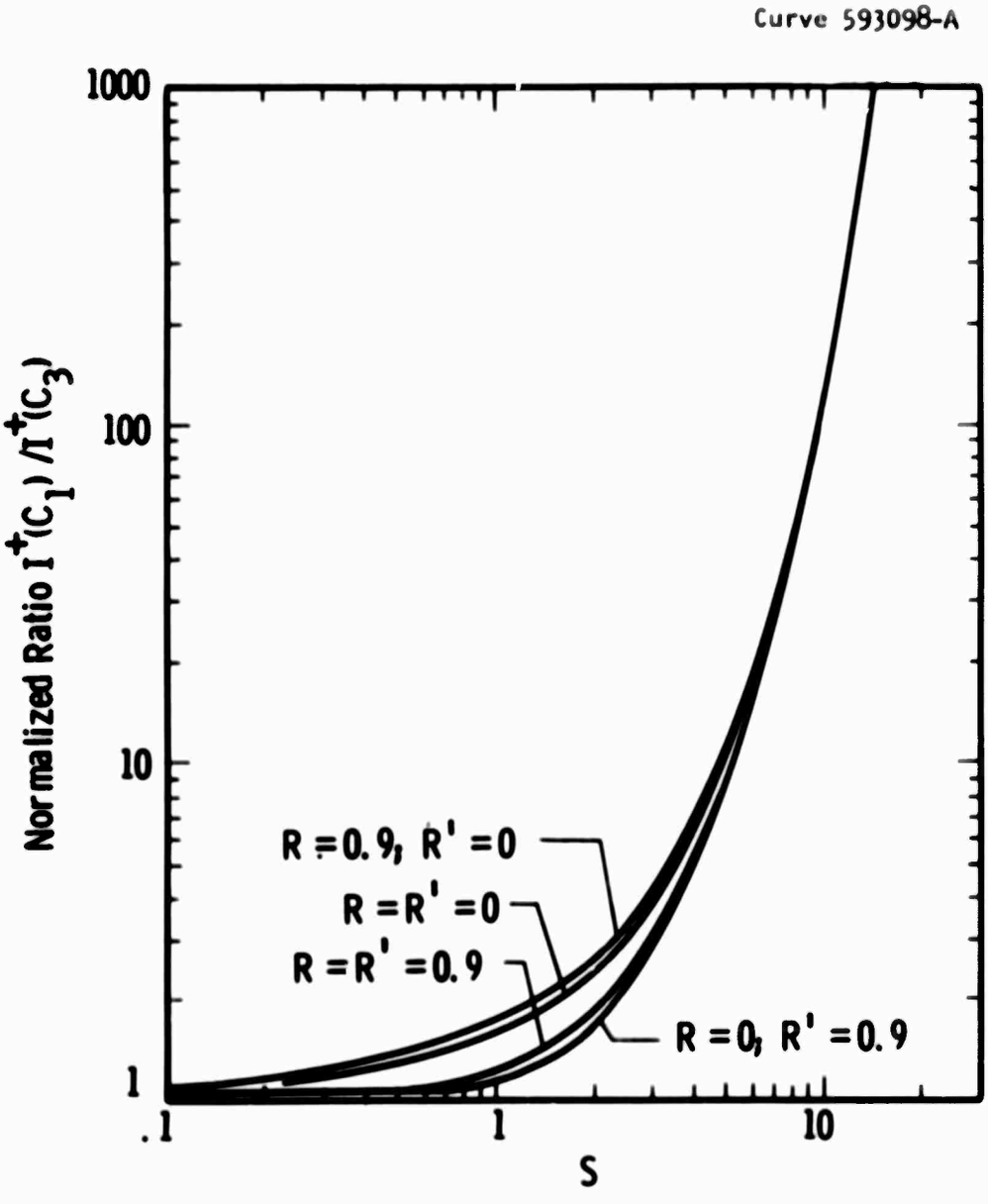

Fig. 6 - The dependence of the computed ion ratio on pressure for the case $\Sigma Q_x/(Q_m + \Sigma Q_x) = 0.1$ showing the dependence of the shape on the reflection coefficients R, R' at the entrance and exit boundaries.

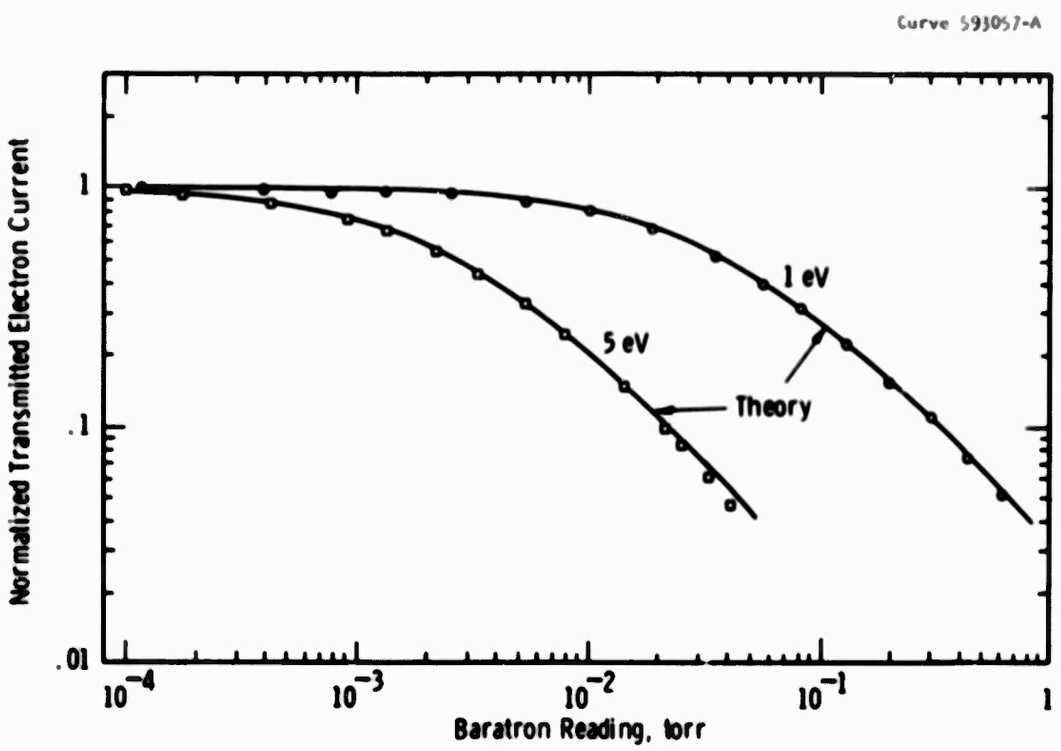

Fig. 7 - Pressure dependence of the transmitted electron current in Xe at the energies indicated. The positions of the exact computed curves relative to the pressure scale are chosen to best fit the data, and serve to determine Q_m at each energy.

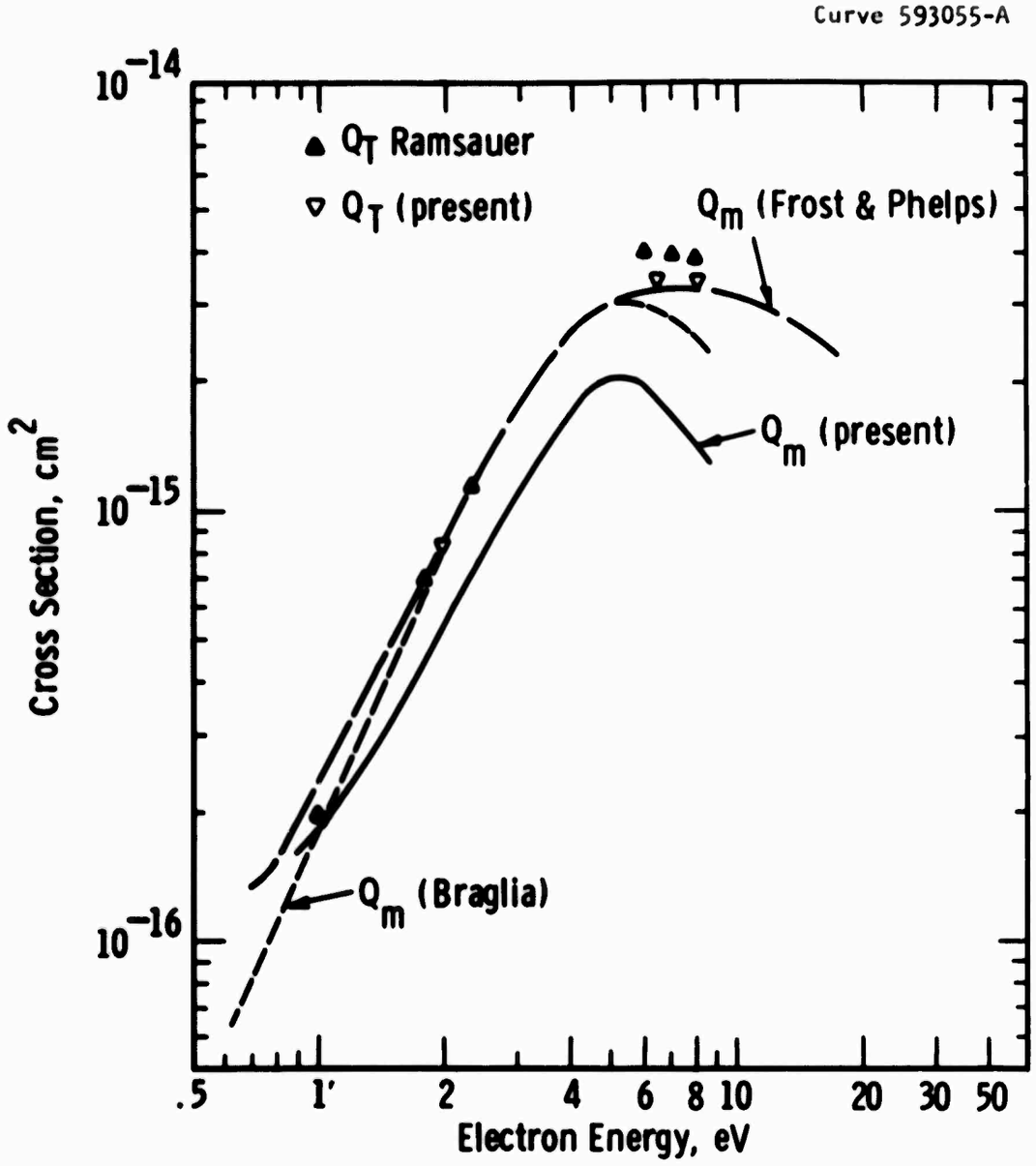

Fig. 8 - The momentum transfer (Q_m) and total (Q_T) cross sections in Xe, as determined in the present work and by previous workers. See discussion in text regarding the discrepancies.

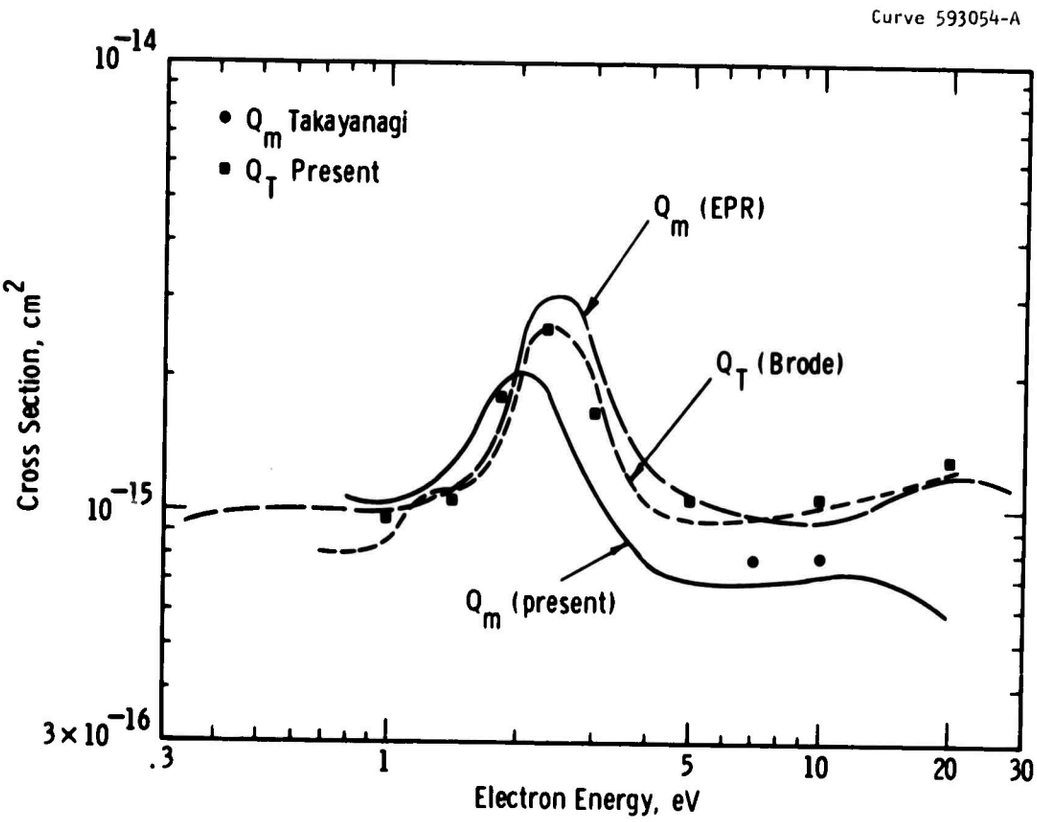

Fig. 9 - The momentum transfer (Q_m) and total (Q_T) cross sections in N_2. The curve labelled EPR is from Ref. 20. See discussion in text regarding the discrepancies.